AN INTERNSHIP REPORT ON

COMPUTATIONAL INVESTIGATION OF STRUCTURAL AND ELECTRONIC PROPERTIES OF CO_2 ADSORBED CORONENE USING DFT

A report submitted in partial fulfilment of the requirements for award of degree of

MASTER OF SCIENCE IN PHYSICS

Submitted by

MALLESH J (U24PG521PHY016)

DEPARTMENT OF PHYSICS

PERIYAR UNIVERSITY

(NAAC A++ Grade-State University-NIRF Rank 59- ARIIA Rank 10) Salem - 636 011, Tamil Nadu, India.

Under the guidance of

Dr. S. VIJAYAKUMAR,

ASSOCIATE PROFESSOR

DEPARTMENT OF MEDICAL PHYSICS

BHARATHIAR UNIVERSITY

(NAAC A++ Grade-State University-21st Rank in MoE- NIRF)

Coimbatore - 641 046, Tamil Nadu, India.

JUNE 2025

BHARATHIAR UNIVERSITY

COIMBATORE - 641 046

(NAAC A++ Grade-State University-21st Rank in MoE- NIRF)

Coimbatore - 641 046, Tamil Nadu, India.

INTERNSHIP CERTIFICATE

This is to certify that the work embodied in the Internship report entitled, "**Computational Investigation of Structural and Electronic Properties of CO_2 Adsorbed Coronene Using DFT**" was carried out by **MALLESH J**, Reg. no: U24PG521PHY016 in the academic year 2025-2026 from 28.05.2025 to 17.06.2025 under the supervision of **Dr. S. VIJAYAKUMAR**, Associate Professor, Department of Medical Physics, Bharathiar University, Coimbatore, Tamil Nadu.

Signature of the Supervisor **Head of the Department**

ACKNOWLEDGEMENT

I wish to express my heartfelt gratitude to Dr. E.K. Girija, Professor and Head, Department of Physics, Periyar University, Salem – 636011, for her kindness and support in allowing me to pursue this valuable internship opportunity.

First and foremost, I would like to convey my sincere thanks to my mentor Dr. J. Kalyana Sundar, Assistant Professor, Department of Physics, Periyar University, Salem, for his invaluable guidance, support, and encouragement throughout my internship. His insights and mentorship have profoundly shaped my professional growth and understanding of the field.

I would like to express my thanks to the internship coordinator Dr. T. Pazhanivel for their support and help in making this internship possible.

I am sincerely thankful to Dr. C. S. Sureka, Associate Professor and Head i/c, Department of Medical Physics, Bharathiar University, Coimbatore, for granting me the opportunity and facilities to pursue my internship in her department.

I am deeply indebted to our internship guide Dr. S. Vijayakumar, Associate Professor, Department of Medical Physics, Bharathiar University, Coimbatore, for his constant support, encouragement, and guidance during this program.

My deep appreciation also goes to Ms. Padmavathy Venkatakrishnan, Ms Asnafarsin Research Scholars, Bharathiar University, Coimbatore, for her persistent support, ideas, and help.

I extend my heartfelt thanks to the research scholars Mrs, Nandhini M, Mr Loganathan S, of the Molecular Designing and Modelling Laboratory, Bharathiar University, Coimbatore, for their constant support and assistance.

I would also like to thank my department staff members and friends who contributed to the successful completion of this internship. Finally, I express my deep gratitude to my beloved family for their blessings and encouragement, which led me to this milestone.

(MALLESH J)

CONTENTS

Computational Investigation of Structural and Electronic Properties of CO_2 Adsorbed Coronene Using DFT

Abstract:

This study presents a comprehensive density functional theory (DFT) analysis of carbon dioxide (CO_2) adsorption on coronene using Gaussian software. The computational investigation employs the B3LYP functional with 6-31G(d) basis set to examine the electronic structure, geometric parameters, and adsorption characteristics of the CO_2-coronene complex. Molecular structures were constructed using ChemCraft software, followed by geometry optimization and electronic property calculations. The results reveal significant changes in bond lengths, HOMO-LUMO energy gaps, and electronic density distribution upon CO_2 adsorption. The bare coronene exhibits a HOMO-LUMO gap of 4.035 eV, which decreases to 2.896 eV upon CO_2 adsorption, indicating enhanced electronic conductivity. CO_2 adsorption on coronene increases its polarizability by 7.47% and strengthens its intermolecular interactions. Adsorption energy calculations suggest weak chemisorption behavior with an adsorption energy of -0.880 eV. Also, the density of states provides the significance of electronic states and the reduction of energy gap due to the adsorption of CO_2 on coronene. The study provides insights into the interaction mechanisms between CO_2 and polycyclic aromatic hydrocarbons, contributing to the understanding of carbon capture materials and surface chemistry phenomena.

Keywords: DFT, CO_2 adsorption, coronene, B3LYP, HOMO-LUMO, chemisorption, Gaussian software, electronic structure

1. Introduction

1.1 Background and Motivation

The increasing atmospheric concentration of carbon dioxide has intensified research into effective CO_2 capture and storage technologies. Polycyclic aromatic hydrocarbons (PAHs) like coronene have emerged as promising candidates for CO_2 adsorption due to their extensive π-electron systems and planar structures. Understanding the fundamental interaction mechanisms between CO_2 and these carbon-based materials is crucial for developing efficient carbon capture systems [6].

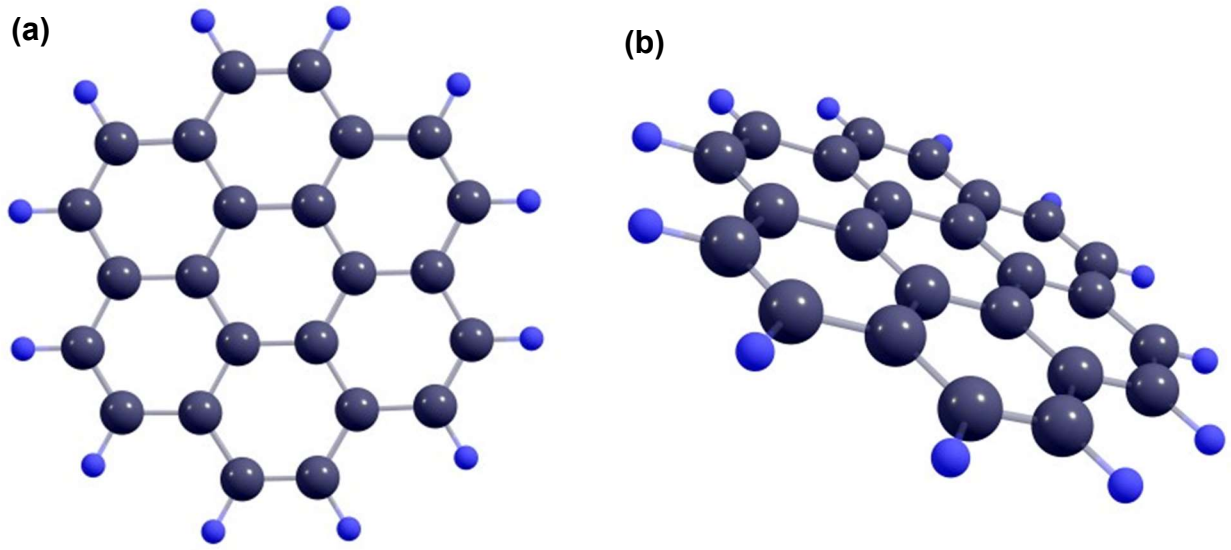

Fig. 1.1 (a) Structure of coronene; (b) Side view of the sheet-like structure of coronene.

Coronene ($C_{24}H_{12}$), also known as super benzene, is a planar circulene consisting of seven peri-fused benzene rings. Its unique aromatic structure and high symmetry make it an excellent model system for studying gas adsorption on graphene-like surfaces. The molecule's extensive conjugated π-system provides multiple potential adsorption sites for small molecules like CO_2.

1.2 Coronene as a Graphene Analog

Coronene serves as an exemplary model system for understanding graphene-like materials due to its extended π-conjugated system and planar geometry. Recent quantum chemical studies

have confirmed coronene's role as a finite-size graphene nanoflake, where electron correlation effects remain significant despite the transition from one-dimensional to higher-dimensional systems. The molecule's electronic structure exhibits characteristics that closely parallel those observed in graphene sheets, making it an invaluable computational model for studying carbon-based nanomaterials.

The analogy between coronene and graphene extends beyond structural similarities to encompass electronic properties. Studies of coronene-derived graphitic nanoribbons have demonstrated how molecular building blocks determine the electronic structure of extended carbon systems [7]. This relationship validates the use of coronene as a representative model for investigating surface chemistry phenomena on graphene-like materials, particularly in the context of gas adsorption and electronic property modulation.

1.3 Applications in Materials Science

Coronene and its derivatives have found extensive applications in organic electronics, particularly in charge-transport materials and electroluminescent devices. The molecule's highly symmetric structure and extended conjugation make it suitable for organic field-effect transistors and other electronic applications. Recent developments have focused on synthesizing coronene-based derivatives with enhanced functionality through strategic substitution and extension of the aromatic framework [8].

The potential applications extend to sensing technologies, where coronene's electronic properties can be exploited for detecting various analytes. Additionally, the molecule's ability to form stable π-π stacking arrangements makes it relevant for supramolecular chemistry and materials design.

1.4 Quantum Mechanics and Computational Chemistry Foundations

The theoretical foundation of this work rests on quantum mechanical principles established in the early 20th century. As Paul Dirac noted in 1929, *the physical laws necessary for understanding chemistry were known, but their application led to equations too complex to solve*

exactly. This challenge gave rise to computational chemistry, which uses approximation methods to solve the Schrödinger equation for many-electron systems.

1.5 Historical Development of Computational Methods

The evolution of computational quantum chemistry represents a remarkable journey from rudimentary approximations to sophisticated methodologies capable of describing complex molecular systems. The development can be traced through several distinct periods, each characterized by specific theoretical advances and computational capabilities.

1.5.1 Semi-Empirical Methods

Semi-empirical quantum chemistry methods emerged as a response to the computational limitations of early quantum mechanical approaches. These methods incorporate numerous approximations and empirical parameters derived from experimental data. The primary motivation for developing semi-empirical methods was to achieve a balance between computational efficiency and reasonable accuracy for large molecular systems.

Semi-empirical methods achieve computational efficiency by parameterizing certain integrals based on experimental data such as ionization energies and dipole moments. While this approach enables calculations on large molecular systems, it introduces limitations in terms of transferability and accuracy for systems dissimilar to those used in parameterization.

1.5.2 Ab Initio Methods

The term "ab initio," meaning "from first principles," was first introduced in quantum chemistry by Robert Parr and coworkers in their study of benzene's excited states. Ab initio methods distinguish themselves by solving the electronic Schrödinger equation using only fundamental physical constants and the positions and number of electrons as input, without relying on empirical parameters.

The development of ab initio methods represented a paradigm shift toward purely theoretical approaches based on quantum mechanical principles. These methods aim to provide accurate

predictions of molecular properties by solving the many-electron Schrödinger equation through systematic approximations rather than empirical fitting.

1.5.3 Born-Oppenheimer Approximation

The Born-Oppenheimer approximation constitutes one of the most fundamental approximations in molecular quantum mechanics. This approximation exploits the significant difference in time scales between electronic and nuclear motion, recognizing that electrons (being much lighter) can rapidly adjust to the slower nuclear movements.

The theoretical foundation rests on the observation that typical bond vibrational motions occur over time scales of approximately 10^{-14} s, while electrons undergo periodic motions within their orbitals on the 10^{-17} s timescale. This three-order-of-magnitude difference in characteristic times justifies treating electronic motion in the field of fixed nuclei. The approximation enables the separation of the total molecular wavefunction into electronic and nuclear components, significantly simplifying the quantum mechanical treatment of molecules.

1.5.4 Hartree-Fock Self-Consistent Field Method

The Hartree-Fock (HF) method, also known as the Self-Consistent Field (SCF) method, represents the cornerstone of modern quantum chemistry. This approach approximates the exact N-body wavefunction using a single Slater determinant of N spin-orbitals for fermions. The method derives its name from the requirement that the final field computed from the charge distribution must be self-consistent with the initially assumed field.

The HF method employs the variational principle to derive a set of N-coupled equations for the N spin orbitals. The iterative solution of these non-linear equations yields the Hartree-Fock wavefunction and energy. While HF theory provides an excellent starting point for more sophisticated methods, it neglects electron correlation effects, which often constitute a significant portion of the total binding energy.

1.5.5 Møller-Plesset Perturbation Theory

Møller-Plesset perturbation theory (MP) addresses the electron correlation deficiency of Hartree-Fock theory by applying Rayleigh-Schrödinger perturbation theory. The method, originally proposed by Christian Møller and Milton S. Plesset in 1934, treats the difference between the exact Hamiltonian and the Fock operator as a perturbation.

The MP approach systematically improves upon the HF solution by calculating energy corrections to various orders: MP2 (second-order), MP3 (third-order), and MP4 (fourth-order). The second-order correction (MP2) represents the most commonly used level, providing a good balance between computational cost and accuracy improvement over HF. The MP2 energy correction specifically accounts for dynamic electron correlation through doubly-excited configurations. While MP methods can provide highly accurate results, convergence issues may arise for systems with small HOMO-LUMO gaps or multireference characters. The Hartree-Fock (HF) method and Post HF methods are limited because it is not based on the Hohenberg-Kohn theorem or Kohn-Sham equations. This leads to systematic errors and unreliable results for many molecular systems, especially in HF method those with significant electron correlation. Density Functional Theory (DFT), founded on these theorems, overcomes these drawbacks and provides greater accuracy for a wider range of chemical problems.

1.6 Density Functional Theory: Exchange-Correlation Functionals

Density Functional Theory emerged as a revolutionary approach through the foundational work of Walter Kohn, Pierre Hohenberg, and Lu Jeu Sham in the 1960s. The fundamental insight of DFT lies in expressing all ground-state properties as functionals of the electron density rather than the many-electron wavefunction, dramatically reducing computational complexity while maintaining chemical accuracy. There are two basic theorems in which DFT is formulated and they are given below,

Hohenberg-Kohn Theorem:

The ground-state electron density uniquely determines all properties of a many-electron system, including its external potential and total energy. There exists a universal energy

functional of the electron density, $E[\rho]\}$, that gives the ground-state energy when evaluated at the true ground-state density. The ground-state energy is found by minimizing this functional:

$$E_0 = \min_{\rho}\{ E[\rho]\}$$

Kohn-Sham Equation:

The interacting many-electron system is mapped to a fictitious system of non-interacting electrons that yields the same ground-state density. The Kohn-Sham equations are solved for single-electron orbitals, whose density reproduces the true electron density.

The Kohn-Sham equation is:

$$\left[-\frac{1}{2}\nabla^2 + V_{\text{eff}}(\mathbf{r})\right]\psi_i(\mathbf{r}) = \epsilon_i\psi_i(\mathbf{r})$$

where V_{eff} includes the external, Hartree, and exchange-correlation potentials.

1.6.1 Advantages of DFT over Traditional Methods

DFT offers several compelling advantages over wavefunction-based methods. It focuses on electron density rather than wavefunction of electrons. Furthermore, DFT inherently includes electron correlation effects through the exchange-correlation functional, unlike Hartree-Fock theory which completely neglects correlation.

The exchange-correlation functional in DFT serves a dual purpose: the exchange component accounts for the antisymmetric requirement of the electronic wavefunction, while the correlation component captures dynamic electron interactions. This unified treatment enables DFT to achieve accuracy comparable to correlated wavefunction methods at a fraction of the computational cost.

1.6.2 Exchange-Correlation Functional Development

The evolution of exchange-correlation functionals follows a systematic hierarchy known as Jacob's ladder.

- The Local Density Approximation (LDA) represents the simplest approach, treating the exchange-correlation energy as if the electron density were locally uniform. While LDA provides qualitatively correct results for many systems, it tends to underestimate exchange effects and overestimate correlation contributions.
- Generalized Gradient Approximation (GGA) functionals improve upon LDA by incorporating density gradients, leading to more accurate descriptions of molecular systems. The GGA exchange hole provides a more realistic representation of the exact exchange hole near the reference electron compared to the more diffuse LDA hole. This improvement results in better bond lengths, atomization energies, and barrier heights for chemical reactions.
- Hybrid functionals incorporate exact Hartree-Fock exchange. The B3LYP functional, combining Becke's three-parameter exchange with Lee-Yang-Parr correlation, exemplifies the hybrid approach and remains one of the most widely used functionals in quantum chemistry due to its robust performance across diverse chemical systems [5].

1.7 Basis Sets

1.7.1 Basis Set Fundamentals

Basis sets constitute the mathematical foundation for expressing molecular orbitals as linear combinations of atomic orbitals. The choice of basis set critically affects both computational efficiency and accuracy, requiring careful consideration of the chemical system and desired properties. Gaussian-type orbitals (GTOs) have become the standard choice due to their computational advantages in evaluating multi-center integrals.

The balance between accuracy and computational cost remains a central consideration in basis set selection, with larger basis sets generally providing higher accuracy at increased computational expense.

1.7.2 The 6-31G(d) Basis Set

The 6-31G(d) basis set employed in this study represents a split-valence basis set with polarization functions. The notation "6-31G" indicates that core orbitals are described by six

primitive Gaussian functions, while valence orbitals are split into inner (three primitives) and outer (one primitive) components. The "(d)" designation signifies the inclusion of d-type polarization functions on heavy atoms, essential for accurately describing molecular geometries and chemical bonding.

This basis set provides an excellent compromise between computational efficiency and chemical accuracy for organic molecules. The inclusion of polarization functions enables the description of molecular anisotropy and is particularly important for systems involving lone pairs or π-bonding interactions [4].

1.8 Functional - B3LYP

The B3LYP functional represents a hybrid approach combining exact Hartree-Fock exchange with DFT exchange-correlation functionals. Despite some known limitations, B3LYP remains the most popular density functional in chemistry due to its good balance of accuracy and computational efficiency. The functional has been extensively validated for organic molecules and shows reliable performance for geometry optimizations and energy calculations [2].

1.9 HOMO-LUMO Interactions and Frontier Molecular Orbital Theory

1.9.1 Fundamental Concepts

The Highest Occupied Molecular Orbital (HOMO) and Lowest Unoccupied Molecular Orbital (LUMO) collectively constitute the frontier orbitals, which play crucial roles in determining molecular reactivity and electronic properties. The energy difference between these orbitals, known as the HOMO-LUMO gap, serves as a key indicator of molecular stability, conductivity, and optical properties.

Frontier Molecular Orbital Theory, developed by Kenichi Fukui and later recognized with the Nobel Prize in Chemistry, provides a framework for understanding chemical reactivity through HOMO-LUMO interactions. The theory posits that chemical reactions primarily involve interactions between the HOMO of one molecule and the LUMO of another, with the orbital overlap determining reaction feasibility.

1.10 Adsorption: Physisorption and Chemisorption

Understanding the nature of gas-surface interactions requires distinguishing between physisorption and chemisorption. These two mechanisms differ fundamentally in their binding forces and characteristics [1]:

- **Physisorption** involves weak van der Waals forces with typical binding energies of 20-40 kJ/mol. It is generally reversible, non-specific, and favored at low temperatures.
- **Chemisorption**, in contrast, involves chemical bond formation with binding energies of 80-240 kJ/mol. It is typically irreversible, highly specific, and favored at higher temperatures.

1.11 Scope and Objectives of This Work

This computational study aims to elucidate the fundamental interactions between CO_2 and coronene through comprehensive DFT analysis. The primary objectives include:

1. **Geometric Analysis**: Determination of optimal adsorption configurations and structural distortions upon CO_2 binding
2. **Electronic Structure Investigation**: Analysis of HOMO-LUMO energy changes and orbital redistribution
3. **Energetic Characterization**: Calculation of adsorption energies and determination of binding mechanisms
4. **Polarizability Studies**: Investigation of electronic response property changes upon adsorption
5. **Mechanistic Understanding**: Classification of adsorption type and identification of key interaction factors

The scope encompasses both bare coronene characterization and detailed analysis of the CO_2-coronene complex, providing insights relevant to carbon capture applications and surface chemistry understanding.

1.12 Computational Methodology Employed

This study utilizes Density Functional Theory with the B3LYP hybrid functional and 6-31G(d) basis set implemented in Gaussian software. Molecular structures were constructed using ChemCraft software, followed by geometry optimization with frequency calculations to confirm stationary points. Electronic structure analysis includes population analysis and DOS.

The CO_2-coronene complex calculations incorporate basis set superposition error correction through the counterpoise method to ensure accurate interaction energies. This comprehensive computational approach enables detailed characterization of the adsorption system and provides reliable data for mechanistic interpretation.

2. Methodology

2.1 Software and Computational Setup

The computational workflow employed two primary software packages: ChemCraft for molecular structure construction and visualization, and Gaussian for quantum chemical calculations. ChemCraft was selected for its intuitive user interface and comprehensive molecular modeling capabilities. Gaussian software was chosen for its robust DFT implementation and extensive basis set library.

2.2 Molecular Structure Preparation

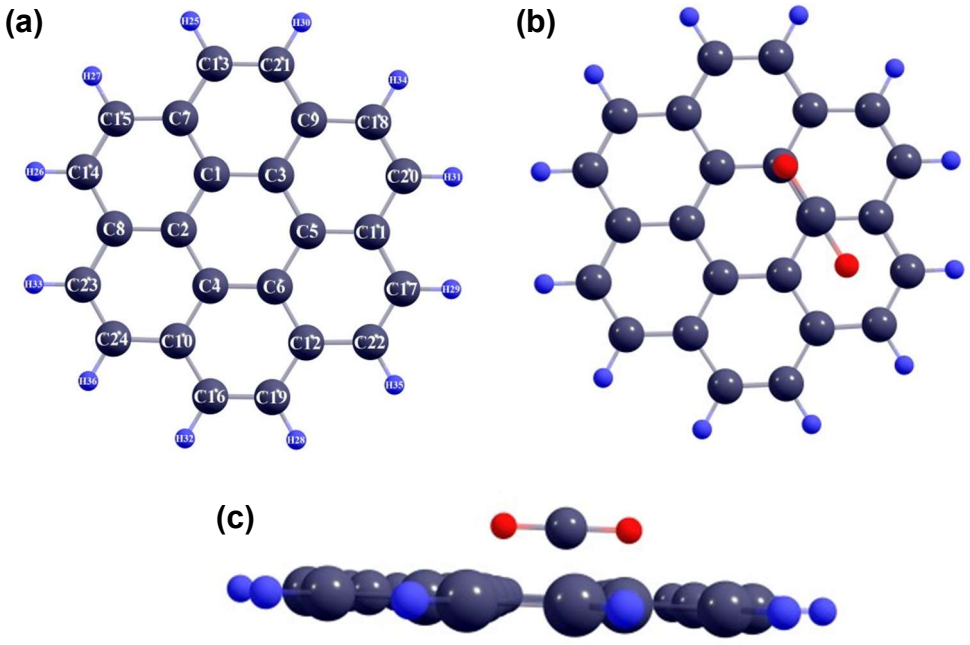

Fig. 2.19 (a) Bare coronene; (b) Horizontal view of CO_2 placed on bare coronene; (c) Vertical view of CO_2 placed on bare coronene.

Initial molecular structures were constructed using ChemCraft's molecular builder tools. The coronene structure ($C_{24}H_{12}$) was built by assembling seven benzene rings in the characteristic peri-fused arrangement. The CO_2 molecule was positioned at around 1.34 Å above the centre benzene ring of coronene surface with the carbon atom placed directly above the C5 carbon of coronene, one oxygen (O1) above C3, and the second oxygen (O2) extending outward.

2.3 Gaussian DFT Calculations

2.3.1 Geometry Optimization

Geometry optimizations were performed using the following Gaussian input specifications:

 # opt freq b3lyp/6-31g(d) geom=connectivity scf=xqc

This calculation setup includes:

- **opt**: Geometry optimization to find minimum energy structures
- **freq**: Frequency calculations to confirm stationary points and calculate thermodynamic properties
- **b3lyp/6-31g(d)**: B3LYP functional with 6-31G(d) basis set
- **geom=connectivity**: Explicit specification of atomic connectivity
- **scf=xqc**: Enhanced SCF convergence algorithm for difficult cases

2.3.2 Electronic Structure Analysis

For bare coronene electronic structure analysis:

 # b3lyp/6-31g(d) pop=(full,nbo) geom=connectivity scf=xqc gfinput

Key features include:

- **pop=full**: Complete population analysis including molecular orbital coefficients
- **nbo**: Natural bond orbital analysis
- **gfinput**: Generation of formatted checkpoint file information

2.3.3 Counterpoise Correction

For the CO_2-coronene complex, basis set superposition error (BSSE) was addressed using counterpoise correction:

 # b3lyp/6-31g(d) pop=full geom=connectivity counterpoise=2 gfinput iop(3/33=1,3/36=-1) scf=xqc

The counterpoise correction addresses the artificial stabilization that occurs when basis functions of one fragment improve the description of another fragment. This method calculates the interaction energy by performing separate calculations on each fragment in the presence of ghost atoms from the other fragments. The **counterpoise=2** keyword indicates a two-fragment calculation (CO_2 and coronene), while the **iop** parameters provide additional SCF control for complex systems [3].

2.4 Property Calculations

2.4.1 HOMO-LUMO Analysis

Highest Occupied Molecular Orbital (HOMO) and Lowest Unoccupied Molecular Orbital (LUMO) energies provide crucial information about electronic properties and chemical reactivity. The HOMO-LUMO gap correlates with electronic conductivity, chemical stability, and optical properties.

2.4.2 Density of States (DOS)

Density of states calculations reveal the distribution of electronic states as a function of energy. DOS analysis provides insights into the electronic structure changes upon adsorption and helps understand the nature of electronic interactions.

2.4.3 Adsorption Energy Calculation

The adsorption energy was calculated using the standard formula:

$$\mathbf{E_{ads} = E_{complex} - E_{coronene} - E_{CO_2}}$$

Where $E_{complex}$ is the total energy of the CO_2-coronene system, $E_{coronene}$ is the energy of isolated coronene, and E_{CO_2} is the energy of isolated CO_2. Negative adsorption energies indicate favorable (exothermic) adsorption processes.

3. Results and Discussion

The optimized structure of the CO_2-adsorbed coronene complex reveals a distinct adsorption geometry where the CO_2 molecule is positioned above the central benzene ring of coronene. Specifically, the carbon atom of CO_2 is located directly above the C5 carbon of coronene, while one oxygen atom (O1) is placed above the C3 carbon. Notably, the adsorption is not limited to non-covalent interactions; there is clear evidence of a bond formation between the carbon atom of CO_2 and the O1 atom, bridging the C5 and C3 carbons of coronene. This configuration leads to a localized interaction site at the center of the coronene, resulting in significant structural and electronic perturbations in the vicinity of the adsorption site.

3.1 Bond Length Analysis

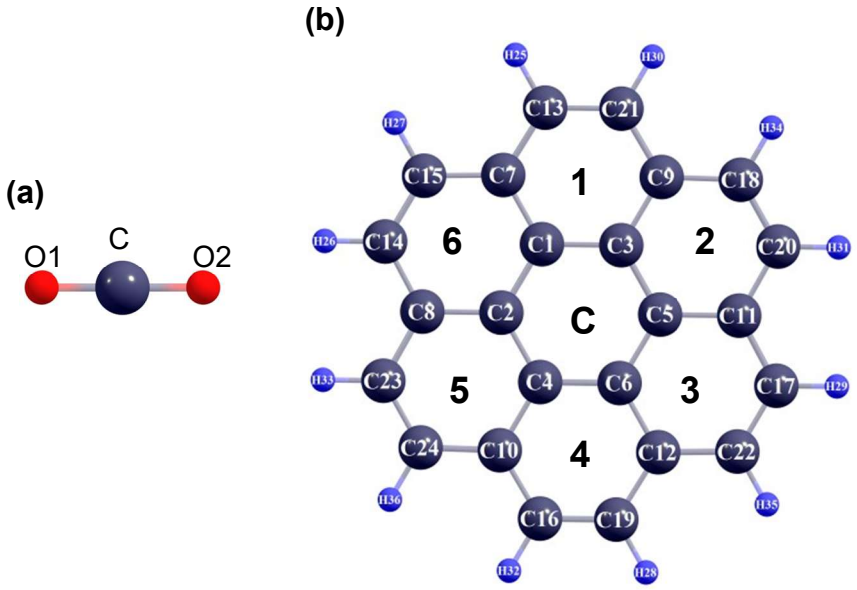

Fig. 3.1 (a) Structure of CO_2 with atom number markings; (b) Structure of coronene showing benzene rings and atom number markings.

CO_2 adsorption induces significant changes in the bond structure of coronene. C–C bonds near the adsorption site show both increases and decreases in length; for example, the C3–C5 bond increases by up to 9.52% while the C11–C20 bond decreases by 3.50%. C–H bonds remain relatively stable, with minimal change (< 0.1%). However, when considering the overall structure

after adsorption, the C–O bond in CO_2 (C–O1) shows the greatest change, increasing in length by about 14%. Detailed discussions of variations in bond lengths for each bond are presented in the Table 3.1, Table 3.2, Table 3.3 below.

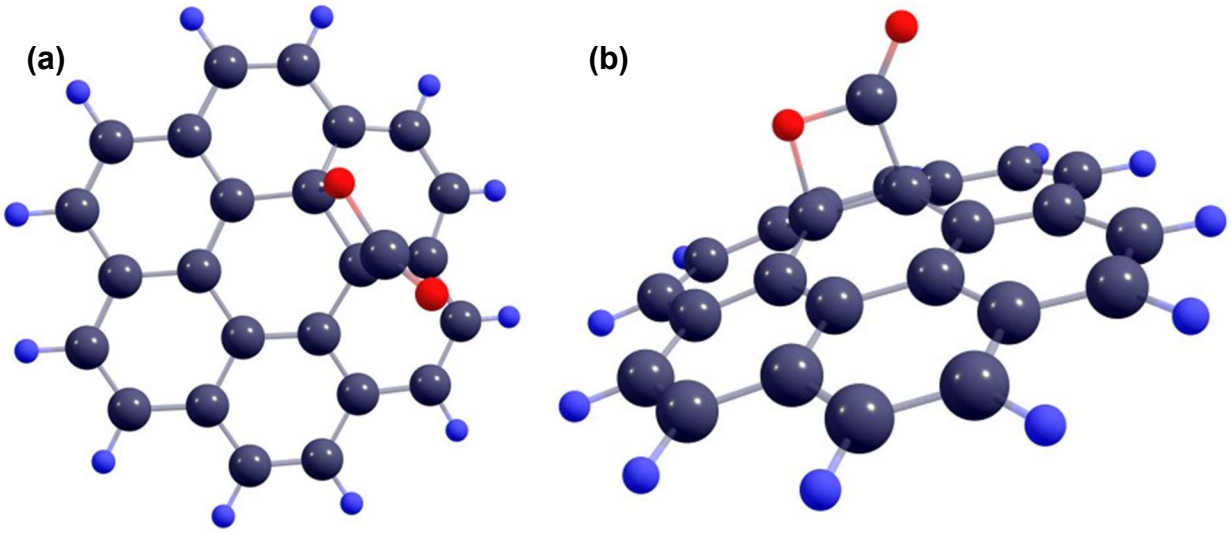

Fig. 3.2 (a) Horizontal view of CO_2-adsorbed coronene; (b) Side view of CO_2 adsorption on coronene.

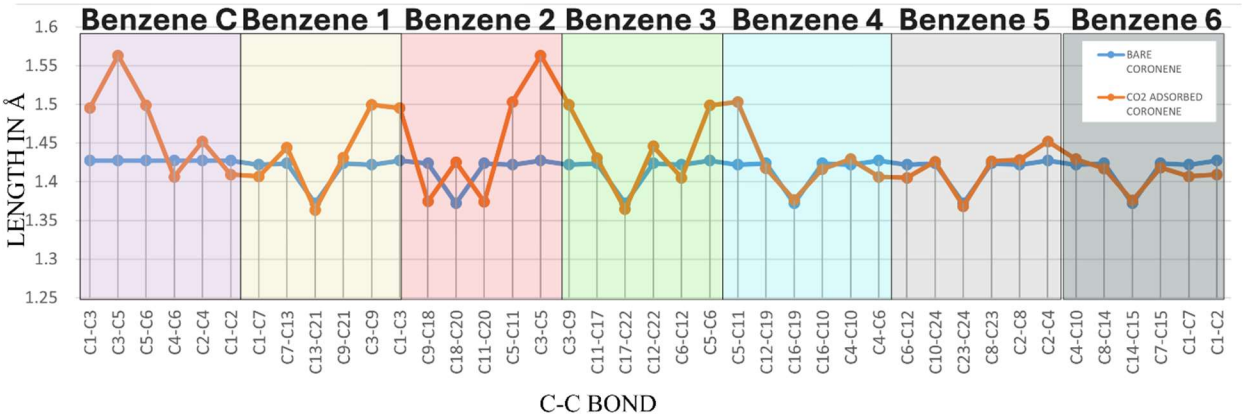

Graph 3.1: Variation in C–C Bond Length in Each Benzene Ring of Coronene After Adsorption where, blue and orange line represents Bare and CO_2-adsorbed coronene respectively.

From the graph 3.1, it can be observed that the most distorted benzene rings were Benzene C and Benzene 2, whereas in Benzene 1 and 3, the bond C3–C9 was disrupted due to its proximity to the binding site. The least distorted structures were Benzene 5 and 6.

Table 3.1 - Summary of Variations in Carbon–Carbon Bond lengths of Coronene in Å

BOND	BARE CORONENE	CO_2 ADSORBED CORONENE	DIFFERENCE IN LENGTH	PERCENTAGE CHANGED
C3-C5	1.42754	1.56341	0.13587	9.517772
C5-C11	1.42212	1.50328	0.08116	5.706973
C3-C9	1.4221	1.49958	0.07748	5.448281
C5-C6	1.42749	1.49867	0.07118	4.986375
C1-C3	1.4275	1.49514	0.06764	4.738354
C18-C20	1.37221	1.42521	0.053	3.862383
C2-C4	1.42754	1.45226	0.02472	1.73165
C12-C22	1.42381	1.44599	0.02218	1.557792
C7-C13	1.4238	1.44428	0.02048	1.438404
C9-C21	1.42385	1.4313	0.00745	0.523229
C4-C10	1.42211	1.42931	0.0072	0.50629
C11-C17	1.42385	1.43075	0.0069	0.484602
C2-C8	1.42211	1.42842	0.00631	0.443707
C16-C19	1.37219	1.37666	0.00447	0.325757
C14-C15	1.3722	1.37577	0.00357	0.260166
C8-C23	1.42383	1.42662	0.00279	0.19595
C10-C24	1.42383	1.42595	0.00212	0.148894
C23-C24	1.37221	1.36831	-0.0039	-0.28421
C7-C15	1.42381	1.41823	-0.00558	-0.39191
C12-C19	1.42381	1.41726	-0.00655	-0.46003
C8-C14	1.42385	1.41708	-0.00677	-0.47547
C16-C10	1.42385	1.41648	-0.00737	-0.51761
C17-C22	1.3722	1.36445	-0.00775	-0.56479
C13-C21	1.37219	1.36363	-0.00856	-0.62382
C1-C7	1.42215	1.40709	-0.01506	-1.05896
C6-C12	1.42215	1.40526	-0.01689	-1.18764
C1-C2	1.42749	1.4094	-0.01809	-1.26726
C4-C6	1.4275	1.40642	-0.02108	-1.47671
C9-C18	1.42383	1.3745	-0.04933	-3.4646
C11-C20	1.42383	1.374	-0.04983	-3.49972

Table 3.2 - Summary of Carbon-Oxygen Bond lengths of CO_2 in Å

BOND	BARE CO_2	CO_2 ADSORBED CORONENE	DIFFERENCE IN LENGTH	PERCENTAGE CHANGED
C-O1	1.18791	1.35411	0.1662	13.99095891
C-O2	1.18792	1.19216	0.00424	0.3569263923

Table 3.3 - Summary of Carbon-Hydrogen Bond lengths of Coronene in Å

BOND	BARE CORONENE	CO_2 ADSORBED CORONENE	DIFFERENCE IN LENGTH	PERCENTAGE CHANGED
C18-H34	1.08746	1.08819	0.00073	0.06712890589
C21-H30	1.08747	1.08754	0.00007	0.00643695918
C14-H26	1.08747	1.08727	-0.0002	-0.01839131194
C17-H29	1.08747	1.08725	-0.00022	-0.02023044314
C23-H33	1.08746	1.08724	-0.00022	-0.02023062917
C20-H31	1.08746	1.08722	-0.00024	-0.02206977728
C15-H27	1.08746	1.08716	-0.0003	-0.0275872216
C22-H35	1.08746	1.0871	-0.00036	-0.03310466592
C19-H28	1.08746	1.08708	-0.00038	-0.03494381403
C16-H32	1.08747	1.08709	-0.00038	-0.03494349269
C24-H36	1.08747	1.08709	-0.00038	-0.03494349269
C13-H25	1.08746	1.08677	-0.00069	-0.06345060968

Table 3.4 - Average Change in Bond Length lengths in Å

System	Bond length (Å)		
	C-C	C-H	C-O
CO_2	-	-	1.188
Coronene	1.414	1.087	-
Co Adsorbed Coronene	1.426	1.087	1.273

The table 3.4 shows that the average C–C bond length in coronene increases slightly from 1.414 Å to 1.426 Å upon CO_2 adsorption, while the average C–H bond length remains nearly constant at 1.087 Å. Additionally, a new C–O bond of forms upon CO_2 binding. The original C–O bond length in CO_2 was increased to 1.273 Å from 1.188 Å.

3.2 Electronic Structure Changes

3.2.1 HOMO-LUMO Modification:

The most significant electronic change upon CO_2 adsorption is the dramatic reduction in the HOMO-LUMO gap from 4.035 eV to 2.896 eV.

Table 3.4 - Summary of HOMO, LUMO and Energy Gap

SYSTEM	HOMO (eV) [MO num]	LUMO (eV) [MO num]	Energy Gap (eV)
Coronene (Bare)	-5.450211364 [78]	-1.415 [79]	4.035
CO_2 Adsorbed Coronene	-5.308 [89]	-2.413 [90]	2.896

From the Table 3.4, it is seen that HOMO energy shifts from -5.450 eV to -5.308 eV, while the LUMO energy decreases more substantially from -1.415 eV to -2.413 eV. This pattern suggests that CO_2 adsorption primarily affects the unoccupied states, consistent with electron density transfer from coronene to CO_2.

This 28% decrease indicates [5]:

- Enhanced electronic conductivity of the complex
- Increased chemical reactivity
- Stronger electronic coupling between CO_2 and coronene

3.2.2 Orbital Redistribution:

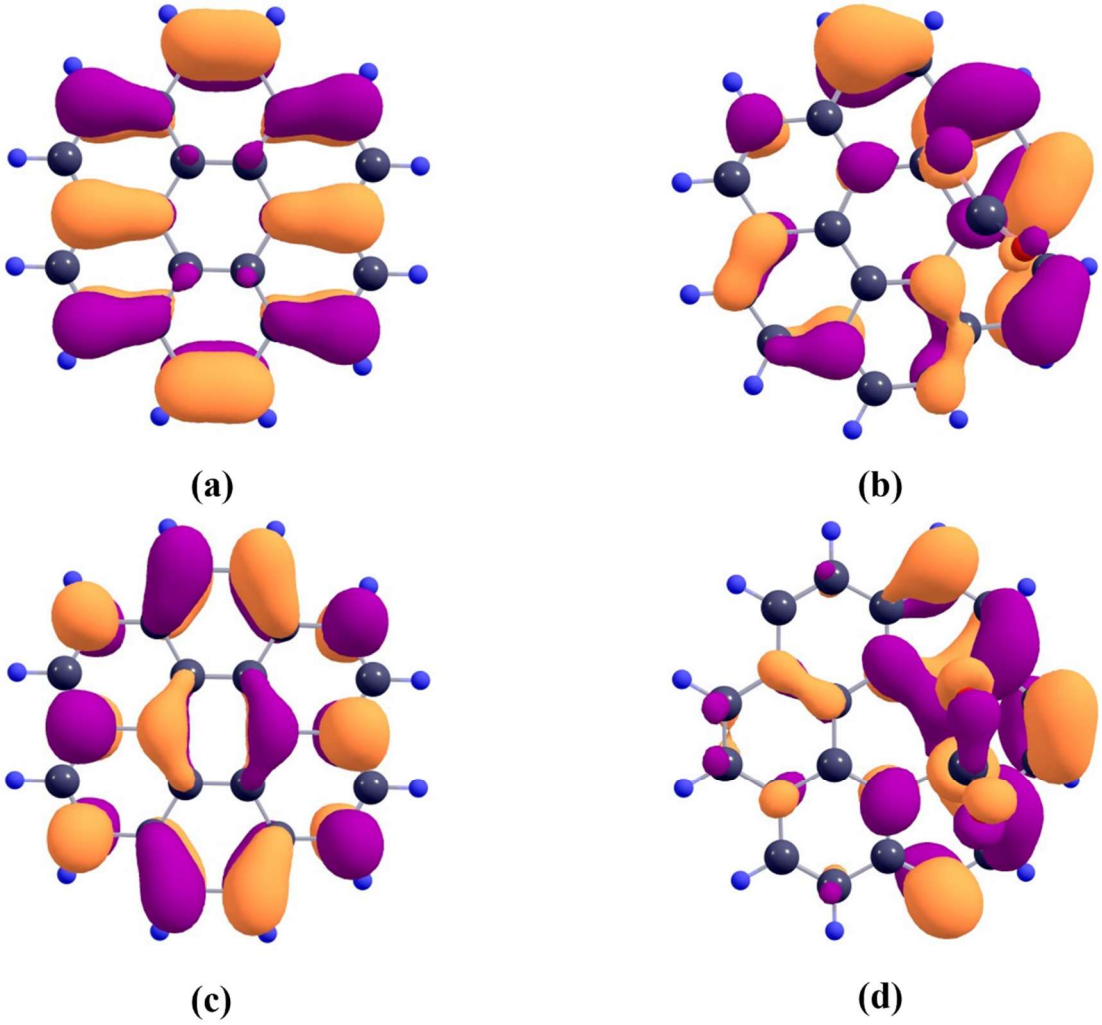

Fig 3.3 (a)HOMO of Bare Coronene; (b)HOMO of CO_2 adsorbed Coronene; (c)LUMO of Bare Coronene; (d)LUMO of CO_2 adsorbed Coronene

The shift in frontier orbitals toward the adsorption site indicates localization of electronic density at the binding region. This orbital redistribution supports the chemisorption mechanism and explains the observed geometric distortions [5].

3.3 Polarizability Enhancement

Upon CO_2 adsorption, the molecular polarizability increases from 7242.042 eV to 7783.086 eV, reflecting an absolute increase of about 7.47%. This enhancement indicates greater electronic delocalization and a larger effective molecular volume of the complex. The polarizability increase

indicates enhanced response to external electric fields and stronger intermolecular interactions, consistent with the formation of a stable adsorption complex [1].

3.4 Adsorption Geometry and Binding Configuration

The optimized CO_2-coronene complex shows a specific binding configuration where the CO_2 carbon atom is positioned 1.575 Å above the C5 carbon of coronene. The O1 oxygen atom is located 1.523 Å above the C3 carbon, while the O2 oxygen extends outward at an angle of 128.907°. This non-linear CO_2 configuration suggests significant interaction with the coronene π-system.

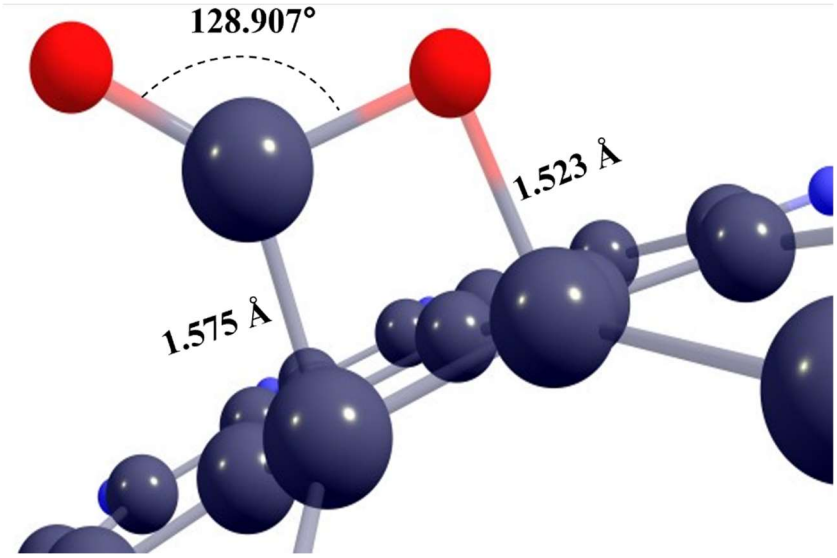

Fig. 3.4: Close-up View of CO_2 Adsorption.

The adsorption height of approximately 1.5-1.6 Å indicates close proximity between CO_2 and the coronene surface, characteristic of chemisorption rather than physisorption. Typical physisorption distances are generally greater than 3 Å, while chemisorption occurs at shorter distances [1].

3.4.1 Adsorption Energetics and Mechanism Classification

The calculated adsorption energy of -0.880 eV (-85 kJ/mol) confirms thermodynamically favorable CO_2 binding. Based on comprehensive analysis of geometric, electronic, and energetic

parameters, the CO_2-coronene interaction is classified as weak chemisorption, combining sufficient binding strength with potential reversibility suitable for practical applications.

Table 3.5: Overview of Adsorption Energy and Adsorption Height

PARAMETER	VALUE
Adsorption energy	-0.880 eV (-85 kJ/mol)
Adsorption Height	1.549 Å

From the Table 3.5, considering both the adsorption height and adsorption energy, the CO_2–coronene interaction can be classified as weak chemisorption.

Reasons for considering chemisorption [1]:

- Short adsorption distances (1.5-1.6 Å)
- Significant structural distortions in both CO_2 and coronene
- Substantial HOMO-LUMO gap reduction
- Moderate adsorption energy (-0.880 eV)
- Bond formation between the CO_2 carbon and C5 atom, bridging Oxygen O1 and C3 of coronene, is a key feature of the adsorption process.

3.5 Density of States Analysis

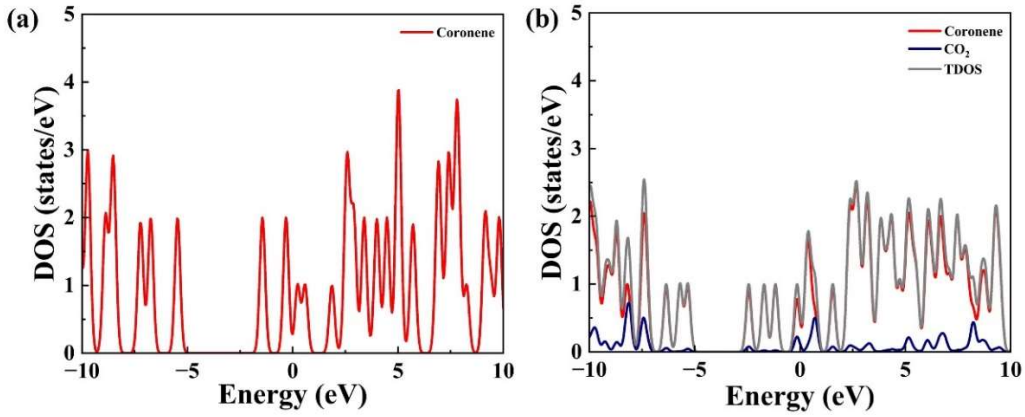

Fig 3.5: Density of states of (a) Bare coronene (b) CO_2 adsorbed coronene where red, navy blue and grey lines denote the DOS of coronene, CO_2 and TDOS of CO_2 adsorbed coronene respectively.

The density of states analysis provides detailed information about electronic structure changes upon CO_2 adsorption. From the fig 3.5, it is evident that the adsorption of CO_2 on coronene has significantly altered the electronic states. Though CO_2 has affected the DOS states, we can comprehend from the fig. 3.5(b) that the TDOS (Total Density of States) and PDOS (Partial Density of States) of coronene have been overlapped, denoting that the adsorption has reduced the electronic states, and the dominating factor of the complex remains with the coronene. Also, the reduction of the energy gap in the adsorbed molecule can be observed by comparing the two figures denoting the efficiency of the CO_2 adsorbed on coronene.

4. Conclusion

This comprehensive DFT study has successfully characterized the interaction between CO_2 and coronene at the molecular level. The following conclusions are drawn:

- ✓ The interaction reveals weak chemisorption behavior with an adsorption energy of -0.880 eV.
- ✓ The investigation demonstrates significant structural changes including bond length variations and atomic displacements, coupled with dramatic electronic modifications reflected in a 28% reduction of the HOMO-LUMO gap from 4.035 eV to 2.896 eV.
- ✓ The 7.47% rise in polarizability upon CO_2 adsorption, reflects enhanced electronic delocalization and stronger interactions. This change underscores the formation of a stable adsorption complex on coronene.
- ✓ The binding geometry shows CO_2 adopting a non-linear configuration with adsorption heights of 1.5-1.6 Å, characteristic of chemisorption interactions.
- ✓ The variation in the DOS states and reduction of the energy gap shows the effect of adsorption of CO_2 on coronene.
- ✓ These findings establish the power of DFT calculations in understanding gas-surface interactions and provide valuable insights for designing CO_2 capture materials based on polycyclic aromatic hydrocarbons.
- ✓ The weak chemisorption behavior identified in the central benzene ring of coronene suggests optimal characteristics for practical CO_2 capture applications, combining sufficient binding strength with potential reversibility.

The study contributes to a fundamental understanding of carbon capture mechanisms and provides a foundation for future research in developing efficient and sustainable CO_2 capture technologies, including structures of coronene doped with other elements.

The comprehensive characterization of electronic, geometric, and energetic properties offers valuable benchmarks for experimental validation and further theoretical investigations in this critical area of environmental chemistry and materials science.

5. References

1. Atkins, P., de Paula, J., & Keeler, J. (2022). *Atkins' Physical Chemistry* (12th ed.). Oxford University Press.
2. Becke, A. D. (1993). Density-functional thermochemistry. III. The role of exact exchange. *The Journal of Chemical Physics*, 5648–5652. doi:10.1063/1.464913
3. Frisch, M. J., Trucks, G. W., Schlegel, H. B., & al.], [. (2016). *Gaussian 16 User's Reference.* Gaussian, Inc.
4. Hehre, W. J., Ditchfield, R., & Pople, J. A. (1972). Self-Consistent Molecular Orbital Methods. XII. Further Extensions of Gaussian-Type Basis Sets for Use in Molecular Orbital Studies of Organic Molecules. *The Journal of Chemical Physics*, 2257–2261. doi:10.1063/1.1677527
5. Jensen, F. (2017). *Introduction to Computational Chemistry (3rd ed.).* Wiley.
6. Kumar, S., & Mishra, A. K. (2022). Modeling the Adsorption of Polycyclic Aromatic Hydrocarbons on Graphynes: An Improved Lennard-Jones Formulation. *The Journal of Physical Chemistry A*, 3567–3577.
7. Ruffieux, P. C. (2012). electronic structure of atomically precise graphene nanoribbons. *ACS Nano*, 6(8), 6930–6935. doi:https://doi.org/10.1021/nn3021376
8. Zeng, Z. W. (2013). Coronenes: Synthesis, Functionalization, and Applications in Organic Electronics and Supramolecular Chemistry. *Chemical Asian Journal*, 8(8), 1680–1691. doi:https://doi.org/10.1002/asia.201300403